Availability of Direct Water-to-Air Optical Wireless Links Through Oceanic Gravity Waves

Pooya Nabavi, Murat Yuksel, and Christopher Kyle Renshaw
University of Central Florida, Orlando, FL USA 32816
pooya.nabavi@knights.ucf.edu, murat.yuksel@ucf.edu, krenshaw@creol.ucf.edu

***Abstract*—Attaining higher speed data communication from underwater to airborne platforms is of high interest for a variety of applications. Existing solutions are cumbersome, involving buoys at the water surface. Direct wireless communication from underwater to an airborne platform using optical beams would resolve several practical issues and potentially enable new wireless applications. We studied the propagation of Gaussian coherent beams from an underwater laser transmitter to a receiver in the open air in the presence of gravity-generated water waves at deep ocean levels. We modeled the emission of coherent Gaussian beams in the presence of third-order Stokes water surface waves. Further, we explored the relationship between beam propagation and turbulence caused by the water waves. The effect of the water wave's steepness and the divergence angle of the underwater laser on the amount of received power was investigated, as well as the link's availability, link power capacity, and survivor analysis of the power collected at the receiver.**

***Index Terms*—Optical beam propagation, visible light, link availability, turbulence, and scattering**

I. Introduction

Over the last two decades, interest in underwater wireless communication has grown due to a variety of factors, including oceanic discoveries, global warming studies, and the requirement for direct connection between underwater (e.g., submarines) and free-space equipment (e.g., ships or communication satellites). The rapid development of autonomous underwater vehicles (AUVs) and unmanned aerial vehicles (UAVs) necessitates the use of reliable telecommunications equipment to facilitate the data exchange between these platforms. Radio waves, which have numerous advantages in free space, are drastically diminished in underwater and water-to-air (W2A) environments, reducing the communication link to a few decameters. Thus, existing underwater wireless communication techniques typically employ sound waves to extend the range of communication; however, this technology is limited to a few hundred KHz and is susceptible to eavesdropping. As Route(B) in Fig. 1 demonstrates, existing solutions employ underwater transmission to a base station on the ocean floor either via radio frequency (RF) or sound waves, followed by optical fiber lines carrying the data signals to a communication relay (buoy) on the water's surface, which then transmits them to the free-space receiver above the water's surface. However, the water surface relay compromises the communication channel's security and significantly increases latency.

This work was supported in part by U.S. Air Force Office of Scientific Research (FA8650-16-D-5408) and National Science Foundation (2120421).

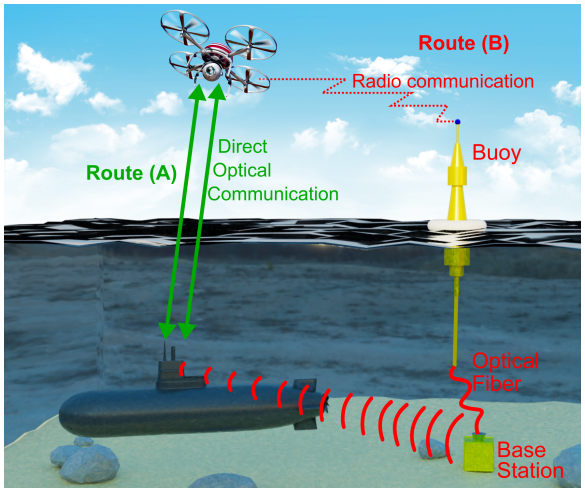

Fig. 1. Two possible routes for communication between a submerged and a free-space vehicle: Route (A): a direct laser communication link; Route (B): a communication link is established through the use of an intermittent buoy on the surface water, exposing the link to eavesdropping.

As an emerging alternative, underwater optical wireless communication (UOWC) utilizes light to provide extraordinarily high bandwidth and minimal latency at low power consumption and long range. This alternative method, as Route(A) in Fig. 1 illustrates, can enable a direct W2A communication link between underwater transmitters and free-space receivers if the designer is able to determine the scattering and level of signal attenuation caused by water waves at the water-air interface. By predicting scattering and signal attenuation in W2A channels, efficient detection algorithms and intelligent transmitter-receiver alignment mechanisms are conceivable. Light waves (in the blue-green wavelength range) are a reasonable compromise because they propagate with relative clarity down to 100 meters in seawater, and laser free-space optical communication (FSOC) can provide gigabit data rates, making them a viable option for AUV-UAV data exchange. Nonetheless, atmosphere and ocean wave turbulence are major impediments along the optical data path, as they can distort the wavefront greatly due to refractive index heterogeneity.

Absorption, scattering, and turbulence all contribute to the degradation of light wave propagation in W2A communication routes, weakening the waves, causing inter-symbol interference, and resulting in information-carrier optical signal fading. A significantly more degrading factor for optical waves in W2A channels is the presence of wavy water surfaces at

the water-air interface, which, due to their complex physical structure, unpredictably scatter and weaken optical signals sent from an underwater source to a free-space receiver. In this work, we explore the feasibility and performance of W2A optical wireless communication (OWC) links.

Contributions. Our contributions include the followings:

- We analyzed a W2A OWC channel using a series of simulations utilizing mathematical models for water gravity surface waves. The modeling effort takes into account the structural properties of the water waves on the deep ocean surface for a better understanding of their impact on laser signal propagation.
- Considering the deep ocean environment, we modeled the optical signals carrying data from a laser transmitter to a free-space photo-detector (PD) and simulated the optical signals using ray-tracing. The model considered gravitational water waves on ocean surfaces and fluid dynamics using third-order Stokes wave equations.
- For an OWC channel between an underwater transmitter and a free-space receiver, we performed statistical analysis of the optical power received by the free-space receiver, and characterized the light intensity decrease caused by the flow and periodic movement of deep-water surface waves, as well as the relationship between sensitivity and availability of the W2A OWC link.
- Using simulation software, we assessed the efficacy of Gaussian laser propagation in direct vertical W2A links.
- We explored the availability of the W2A communication link and the influence of various PD setups on the free-space receiver. Additionally, we analyzed the maximum receiving power capacity available in such W2A links.

Paper Organization. The remainder of this study is organized as follows: Section II provides an overview of existing literature on the concept of water-to-air UOWC. In Section III, we simulate and discuss the propagation of data-carrying Gaussian rays through water waves created by the Earth's gravity at deep oceanic surfaces. Section IV delves into detail about the simulation results and summarizes the findings.

II. Related Work

Underwater optical wireless communication (UOWC) has garnered considerable attention in the last decade due to its higher-than-Gbps data rates, and several experimental studies have corroborated the theoretical results [1]. Most of the UOWC studies explored the models of underwater light absorption, scattering, and scintillation [2], [3] and their effects on underwater communications, as well as the optimal wavelengths for UOWC systems in various waters [4]. Several efforts also looked at the experimental demonstration of UOWC concepts, e.g., using 532nm wavelength LED transmitters to attain Gbps data rate using a laser transmitter over a few meters' link range [5].

Recently, there has been notable work in attaining wireless data transfer from underwater to platforms above the water body. This hybrid method of W2A communication presents a significant obstacle to OWC links at the water-air interface. The water surface waves reflect and scatter signals, resulting in increased energy loss. Although RF waves are relatively efficient at the water-air interface, they are highly absorbed by seawater, reducing communication range to impractical levels [6]. Due to the complexity of the water-air interface's impact on the OWC link, there have been studies of the characteristics of light propagation through the water-air interface [7]–[9]. Studies showed that random surface waves' impact would be negligible for duplex W2A OWC if water depth is appropriate [10], wind-induced distortions on the water surfaces notably affect laser beam optical propagation [7], and transmission power or wind speed reductions impact BER performance on the link in coastal and harbor waters [11]. To understand the effect of ambient light on the receiver PD's operating state (which is mostly assumed linear), [12] evaluated the W2A-OWC interaction in bright light, showing that the noise's impact can be significant. The effect of changing the water surface height on the received beam quality and BER performance was investigated [13].

To address the disturbance on the W2A OWC link, the idea of adding redundant components to the transmitter and/or the receiver was explored. Using an LED array at the transmitter side was shown to be beneficial [14] over a short distance (1.2 m) as well as over longer distances (150 m) if the environment is low light. Placement of under water mirrors [8] to steer more light through the W2A interface showed a notable improvement on the link quality as well.

The complexity of the W2A interface was tackled by interesting combinations of light modulation and optics. Combining space-division-multiplexing (SDM) with pulse amplitude modulation (PAM) was shown to significantly increase the total transmission capacity for red-light vertical-cavity surface-emitting laser (VCSEL) transmitters using two-stage injection locking [15]. Laser transmitters using OFDM were also shown to be effective over short ranges [16]. As an interesting mix of optics and modulation, a pair of plano-convex lenses was positioned in front of an ultraviolet LED, and the LED was modulated with OFDM [17]. The study showed that the lenses combined with OFDM notably helped in reducing the negative impact of the waves, with the FOV being 25°.

The reliability of W2A links received sizable attention. Direct transmission through the W2A interface and retro-reflection of the transmitter beam (based on feedback from the receiver) were compared [18], and it was revealed that retro-reflection reduced the outage probability and BER of the link by 200% and 170%, respectively. The effects of distance, misalignment, and waves on the surface and transparency of the water were investigated by [19]. To evaluate the coverage characteristics of W2A links, a focus-adjustable lens was used in front of a green LED to adjust the beam's divergence [20]. The study demonstrated that due to the random spatial modulation effect of a wavy water surface, the mean channel gain may be greater than that of a calm water surface, particularly when the transmitter and receiver are misaligned.

Our study's key difference from the prior work is its

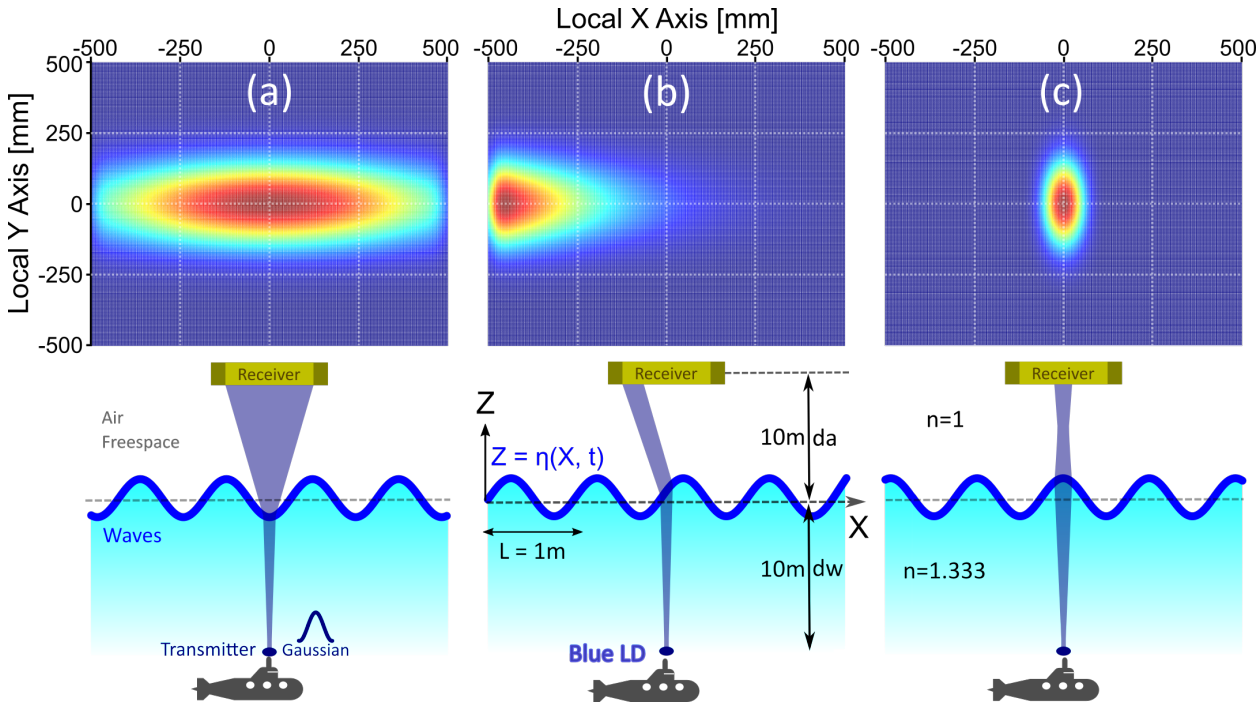

Fig. 2. The effect of water wave motion on the propagation of Gaussian beams carrying data; (a) The water wave acts as a negative-power diverging surface. (b), (c) Water waves have a collimating and converging effect on the wave's propagation.

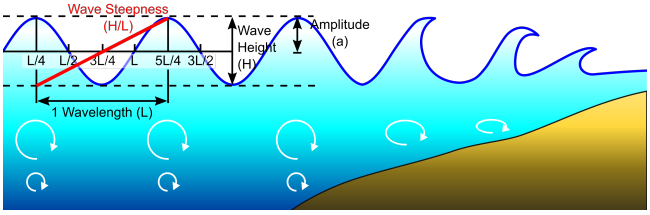

Fig. 3. Illustration of the physical structure and characteristics of third-order stock deep-water waves at the interface between underwater and free space

detailed modeling of the effects of the water surface wave characteristics (e.g., steepness) and transmitted beam's characteristics (e.g., power and divergence angle) on the W2A communication link's availability and capacity. Using coherent ray-tracing, we looked at the spatial properties of the received power. We also explored the impact of receiver combining methods on link reliability.

III. System Setup

Optical links between AUVs and UAVs consist of three parts that critically impact communication performance: The first is the underwater transmitter, the second is the free space (air) and water surface interface with gravity-induced water waves, and the third part is the FSO telecommunication receiver. Oceanic turbulence arising from surface waves is much stronger than atmospheric turbulence and significantly degrades the instantaneous intensity pattern. Since laser beams weaken in shallow sea water, ocean water was studied down to only 10 meters. The transmitter in our system was a coherent Gaussian laser diode located 10 meters below the water surface. Later, the effect of the transmitter divergence angle on Gaussian ray propagation toward a free-space receiver was investigated in the water-air interface.

The free-space receiver was located 10 meters above ocean level. Phase speed and amplitude of nonlinear oceanic surface gravity waves can be estimated using the Stokes perturbative solution of the nonlinear surface gravity wave problem [21]. In fluid dynamics, a Stokes wave is a nonlinear and periodic surface wave on an inviscid fluid layer with a constant mean depth. This modeling approach dates back to the mid-nineteenth century when Sir George Stokes used the perturbation series approach, known presently as the Stokes expansion, to develop approximate solutions for nonlinear wave movement. Stokes wave theory has direct practical applications for medium and deep-water waves and is used for designing coastal and offshore structures to determine wave kinematics (free surface height and flow velocity), which are then used to determine incoming wave loads on the structure being designed. Deep ocean water waves consist of cnoidal waves to which the third-order Stokes wave applies [21]. These waves can be defined as follows [22]:

$$\eta(x,t) = a\Big[[1-\frac{(ka)^2}{16}]\cos(\theta) + \frac{(ka)}{2}\cos(2\theta) + \frac{3(ka)^2}{8}\cos(3\theta)\Big] \quad (1)$$

where $\eta(x,t)$ is the free surface height as a function of horizontal coordinates, x, and time, t. Likewise, ka is the steepness of the wave (slope), a is the first order wave amplitude, and θ is the wave phase defined as $\theta = kx - \omega t$, where $k = 1/\mathrm{L}$ is the wave number, L is the wavelength, and ω is the angular frequency.

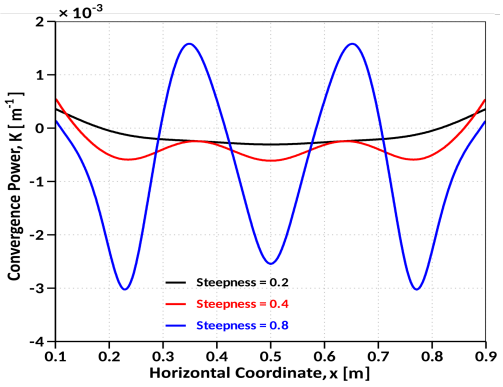

Fig. 4. Equivalent convergence power of third-order stock water wave surfaces at various steepness levels vs. horizontal coordinate.

To determine the radius of curvature and thus the optical power caused by the water surface, we can perform the following calculation:

$$R = \frac{\sqrt[3]{(1+(\frac{\mathrm{d}\eta(x,t)}{\mathrm{d}x})^2}}{\frac{\mathrm{d}^2\eta(x,t)}{\mathrm{d}x^2}} \tag{2}$$

where R denotes the radius of curvature of the water wave at the horizontal coordinate, x, and so the optical convergence power of the water wave at x can be calculated as follows:

$$K = \frac{n_{air} - n_{water}}{R} \tag{3}$$

where K (unit: m^{-1}) denotes the equivalent optical convergence power of the water surface[1] (Fig. 4) and $n_{air} = 1$ and $n_{water} = 1.333$ denote the refractive indices of free space and water, respectively. A positive or negative surface convergence power indicates the water surface wave's convergence or divergence influence on the propagation of incident Gaussian beams in free space. The underwater laser diode, located 10 meters below the water surface, emits a Gaussian beam with 1 watt of power at the wavelength of 450 nm. The free-space receiver is assumed to be installed on a UAV with 1 m^2 cross-section and is perfectly aligned with the line-of-sight of the transmitter. The continuous flow and movement of ocean waves change how coherent Gaussian beams propagate toward the receiver. Depending on the ocean wave's location when in contact, the laser beam can converge to a free-space focal point, diverge or both.

IV. Simulation Result

In this section, following the system setup above, an optical communication link from an underwater transmitter to a free-space receiver was simulated. The effect of the underwater laser transmitter's divergence angle on the free-space receiver's collected energy and the data-carrying beam's propagation from the water-air interface was used to investigate different communication channel scenarios from ocean water waves with different steepness levels and structures due to the Earth's gravity. The third-order Stokes wave equation was used for the mathematical simulation of deep oceanic waves.

[1]The degree to which a surface converges or diverges light is referred to as optical convergence power (also known as dioptric power, refractive power, focusing power, or convergence power).

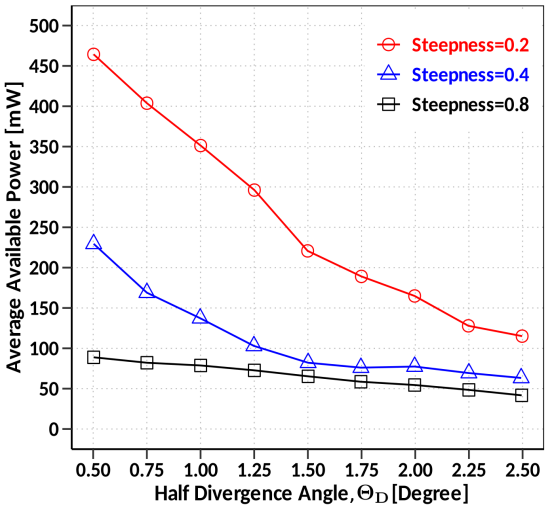

Fig. 5. The effect of the steepness of water waves on the average maximum available power at a free-space receiver for transmit half-divergence angles.

A. Maximum Average Available Power Analysis

Fig. 5 shows the average change of available power in the free-space receiver's 1 m^2 cross-section due to increasing the divergence angle of the laser diode. It also shows the effects of deep ocean surface water waves with different steepness values on the average available power. As shown, increasing the underwater optical transmitter's divergence angle reduced the receiver's average received power, and ocean waves with higher steepness levels severely scattered the light signals hitting the water surface and further dissipated the receiver's average received power. Fig. 5 shows the maximum steepness of 0.8 for the ocean waves. According to [23], this value determines the maximum threshold of ocean waves before breaking wave or whitecapping, and ocean waves with sub-0.88 steepness can be modeled with accurate approximation using the third-order Stokes wave equation.

To calculate the free-space receiver's average received power, the physical structure of deep ocean waves was moved 200 times by an integer multiple of L/200 (where $L = 1m$ is the water wave's wavelength as shown in Fig. 3) to accurately calculate the interaction between the emitted data-carrying laser beam and the water surface, and ultimately obtain average received power by considering every possible interactions between the emitted laser beam and ocean waves. This information was also used to evaluate the performance of different spatial arrangement of photodiodes installed in the UAV to achieve high communication availability in the water-air communication link. Fig. 6 evaluates the effect of movement and the gravitational ocean wave current with various steepness values on instantaneous received power in FSO receivers for underwater laser transmitters with different Gaussian beam divergence angles. According to the horizontal axis of Fig. 6, 200 different ocean wave positions were

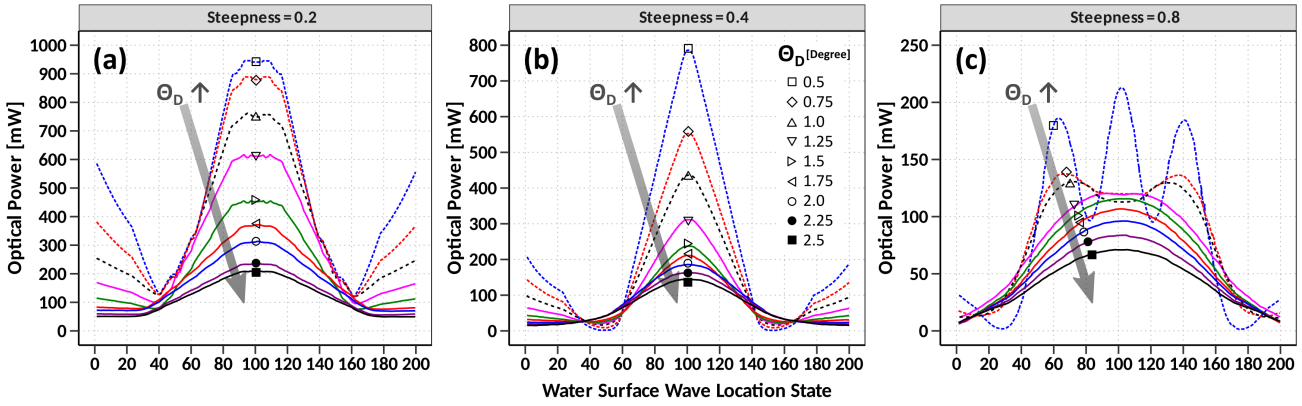

Fig. 6. The impact of the half-divergence angle of the transmitter (i.e., Θ_{D}) on the maximum available power at the 1 m^2 free-space receiver for gravity water waves with varying levels of surface steepness.

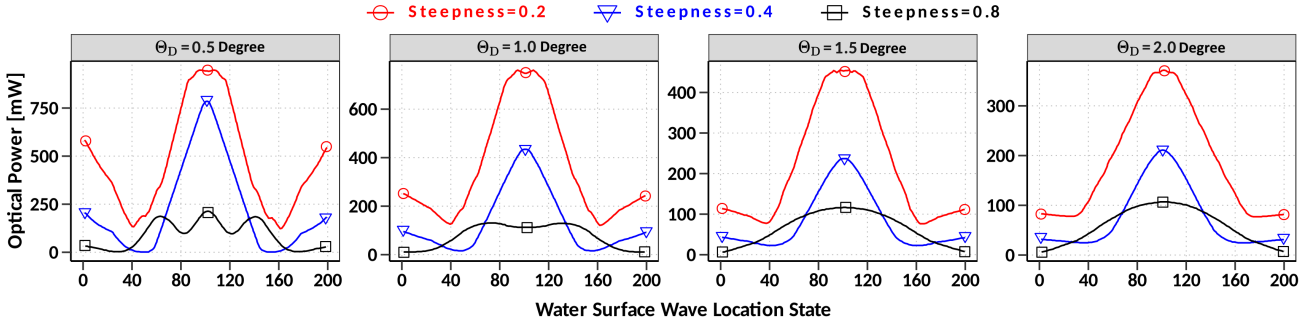

Fig. 7. The tracking of the receiver's instantaneous available optical power as a result of the motion of water surface waves with varying steepness for different transmitter half-divergence angles.

considered, and the underwater laser transmitter with a higher divergence angle reduced the collectable power in the free-space receiver for all the gravitational ocean waves with different steepness levels.

Due to the ocean waves, the laser beams interacting with water surface waves either alternatingly converged (Fig. 2(c)) in the free-space or propagated toward the receiver in a diverging form (Fig. 2(a)). In other words, ocean waves can be seen as a lens with a positive, converging optical power alternatingly changing into negative, diverging optical power due to wave motion. As a result, three scenarios of free-space laser beam propagation could be assumed, depending on the distance between the transmitter and the water surface (which determines the physical beam spot size on the water surface) and the physical shape of the ocean waves colliding with the laser beam on the water surface. In the first scenario (Fig. 2(c)), the transmitted laser beams interact with the ocean waves of positive optical power. In this case, converging laser beams propagated toward the optical communication receiver. The peaks suggest the maximum received optical power in the receiver. In the second scenario (Fig. 2(a)), all the laser beams interact with ocean waves of negative optical power. In such a case, the transmitted power is transmitted in a diverging form in the free space. As a result, a very small portion of the optical power can be collected on a UAV cross-sectional area of 1 m^2. This is evident from the areas of low received optical power in Fig. 6.

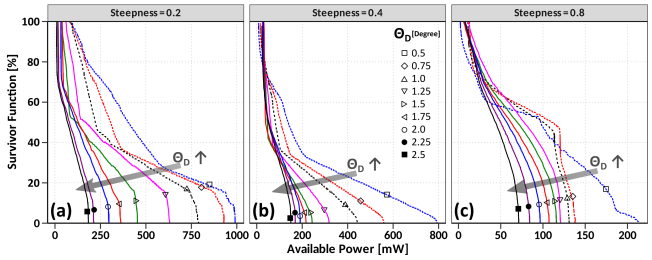

Fig. 8. Survivor analysis of the available power; survivor function; The probability of the available power at the 1 m^2 cross section of the free-space receiver being greater than a specified value for various transmitter half-divergence angles (Θ_{D}) in the presence of water waves of differing steepness levels. The survivor function makes it possible to determine whether or not the maximum available power will survive beyond the specified threshold value.

B. The Effect of the Transmitter Divergence Angle

In the third scenario, at an increased laser divergence angle in the optical transmitter, a fraction of laser beams interact with the converging waves, whereas the remaining waves interact with the diverging ocean waves. An increase in the divergence angle of the underwater transmitting laser increases the spot size of the laser beams colliding with the ocean waves. As a result, the collision's spot size interacts with a mixture of water waves with positive and negative optical convergence powers. This leads to the interference of coherent Gaussian beams and an interferometric pattern in the receiver. Fig. 6(c) depicts the third scenario in the form of sinusoidal optical power

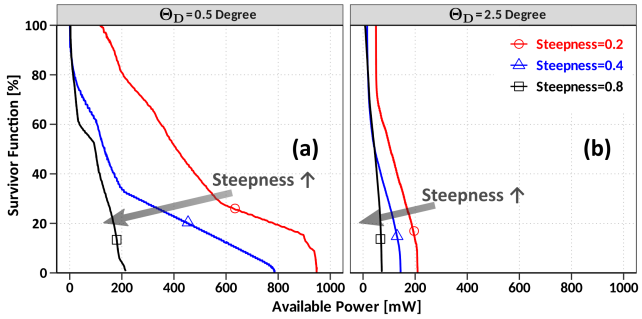

Fig. 9. The effect of the surface steepness of a water wave on the probability of available power at a $1m^2$ free-space receiver surviving and exceeding a threshold for various transmitter half-divergence angles.

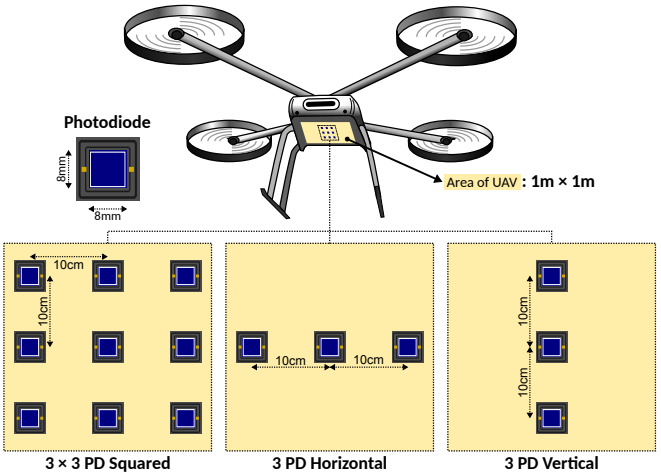

Fig. 10. A setup demonstrating different photodiode arrangements with a 10cm spacing across the UAV's available $1m^2$ cross-section area.

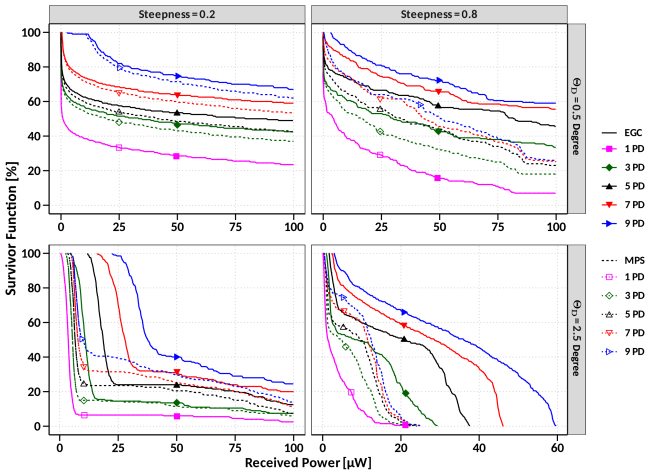

Fig. 11. The statistical survival analysis of received power was performed using a horizontal arrangement of PDs on a free-space receiver, utilizing EGC and MPS PD combination techniques for various transmitter half-divergence angles and water wave steepness levels.

oscillations in the free-space receiver due to the constructive and destructive superimposition of the propagated laser beams at the receiver.

In Fig. 7, for different transmit divergence angles of the Gaussian beam, we plotted the change in the amount of power received at the receiver throughout the full period of flow and movement of water waves. As can be observed, the amount of power received diminished as the divergence angle of the underwater laser increased. Comparing Figs. 7 and 5, it can be seen that, while the average power received at steepness = 0.4 was higher than that received in the steepness of 0.2 (as shown in Fig. 5), tracking the power received when moving ocean waves in Fig. 7 shows that, in some cases of ocean waves, the received power in mode of steepness=0.2 was greater than the received power in mode of steepness=0.4. In Fig. 8, we illustrated the statistical behavior of the maximum available power for collection at the UAV when different transmitter divergence angles were used in conjunction with various water wave steepness values. The survivor function percentage indicates the probability of receiving power greater than a specified threshold and provides insight into the maximum power budget analysis of the link which can be used to design and select appropriate optical transmitters and photodetectors' sensitivity. As shown in Fig. 9, although steepness has a greater effect on beams propagated by laser diodes with a lower divergence angle, choosing a lower divergence angle for the transmitter is preferable to having a higher divergence angle because it results in a higher collectable power at the receiver for all water wave steepness levels.

C. Link Availability Analysis

We analyzed the communication link availability in this subsection by utilizing and arranging PDs on the 1 m^2 cross-section of the free-space UAV. As shown in Fig. 10, we considered the horizontal and squared arrangement of PDs with an aperture area of 8 mm and a spacing of 10cm for the PD arrays with 1, 3, 5, 7, and 9 PDs, respectively. We assumed that each PD in the array had a minimum detectable power[2] of 15 μW and considered two signal combining techniques for combining the received photocurrent outputs of the PDs in the array.

We began by considering the equal gain combination (EGC) technique as a straightforward and well-known receiver combination technique. The primary advantage of the EGC algorithm is that it allows for the collection and superimposition of incident power spread over a larger area of the free-space receiver simply by superimposing photocurrents from all PDs. The primary disadvantage of the EGC algorithm, which limits its application and effectiveness, is that each additional PD

[2]The Noise Equivalent Power (NEP) of a detector is the optical power incident on it that must be applied to equalize the noise power from all sources within the detector; in other words, the NEP is the optical power that results in a signal-to-noise ratio of one. In a nutshell, this is the threshold at which a signal can be detected. Calculating the minimum detectable power, P_{min} is then can be obtained as $NEP(\lambda) \times \sqrt{BW}$.

added to the PD array introduces its own noise into the aggregate output photocurrent received by all the PDs in the array. This raises the question of whether the additional PD can collect enough optical power to compensate for the noise introduced to the aggregate output photocurrent for different transmitter divergence angle and for communication links containing water waves of varying steepness levels. Our analysis established that the answer to the preceding question is negative, indicating that the EGC algorithm will be ineffective at ensuring high link availability especially for large transmit divergence angles. To address this issue, we implemented a superior signal combination technique called maximum power selection (MPS). At any point in time, this algorithm will make a decision at the receiver based on the photocurrent received by the PD that receives the highest level of optical power out of all the PDs in the array and will make a decision based on a signal PD time. We calculated and compared the percentage of available W2A links for both the EGC and MPS algorithms using the received power's survivor function percentage shown in Fig. 11 for various PD setups shown in Fig. 10 and photodiodes with a minimum detectable power of 15 μW. We observed that, regardless of the water surface waves' steepness, the MPS algorithm attains higher than 75% link availability when 9 PDs with a minimum detectable power of 15 μW are utilized. We also observed that EGC's performance in terms of link availability saturates earlier than MPS due to the noise added by each PD.

V. Conclusion and Future Work

We investigated how Gaussian coherent beams propagate from an underwater laser transmitter to an established receiver in the open air in the presence of water waves generated by gravity at deep ocean levels. We modeled the emission of coherent Gaussian beams in the presence of third-order Stokes water waves in the deep ocean. We discussed the connection between beam propagation and the turbulence generated by water waves. We investigated the influence of the steepness of the water waves and the divergence angle of the underwater laser on the amount of receivable power reduction and estimated the probability of the received power collecting at the receiver in the free-space.

This study's key contribution is the characterization of the water-to-air FSO communication channel using detailed models of water surface waves. Various future work dimensions are possible. Our baseline modeling effort can be extended to scenarios involving many randomly generated water surface waves. It will also be worthwhile to study the impact of movements of the free-space receiver, such as vibration and sway. In particular, water waves can propagate at a random angle with respect to the orientation of the free-space receiver which may be attached to a drone.

References

[1] C. Shen, Y. Guo, X. Sun, G. Liu, K.-T. Ho, T. K. Ng, M.-S. Alouini, and B. S. Ooi, "Going beyond 10-meter, Gbit/s underwater optical wireless communication links based on visible lasers," in *IEEE Opto-Electronics and Communications Conference*, 2017, pp. 1–3.

[2] M. V. Jamali, A. Mirani, A. Parsay, B. Abolhassani, P. Nabavi, A. Chizari, P. Khorramshahi, S. Abdollahramezani, and J. A. Salehi, "Statistical studies of fading in underwater wireless optical channels in the presence of air bubble, temperature, and salinity random variations," *IEEE Tran. on Communications*, vol. 66, no. 10, pp. 4706–4723, 2018.

[3] Y. Baykal, "Higher order mode laser beam scintillations in oceanic medium," *Waves in Random and Complex media*, vol. 26, no. 1, pp. 21–29, 2016.

[4] L. J. Johnson, "The underwater optical channel," *Dept. Eng., Univ. Warwick, Coventry, UK, Tech. Rep*, 2012.

[5] H. M. Oubei, J. R. Duran, B. Janjua, H.-Y. Wang, C.-T. Tsai, Y.-C. Chi, T. K. Ng, H.-C. Kuo, J.-H. He, M.-S. Alouini *et al.*, "4.8 Gbit/s 16-QAM-OFDM transmission based on compact 450-nm laser for underwater wireless optical communication," *Optics express*, vol. 23, no. 18, pp. 23 302–23 309, 2015.

[6] Z. Zeng, S. Fu, H. Zhang, Y. Dong, and J. Cheng, "A survey of underwater optical wireless communications," *IEEE communications surveys & tutorials*, vol. 19, no. 1, pp. 204–238, 2017.

[7] O. Alharbi, W. Xia, M. Wang, P. Deng, and T. Kane, "Measuring and modeling the air-sea interface and its impact on FSO systems," in *Laser Communication and Propagation through the Atmosphere and Oceans VII*, vol. 10770, 2018, p. 1077002.

[8] Y. Chen, M. Kong, T. Ali, J. Wang, R. Sarwar, J. Han, C. Guo, B. Sun, N. Deng, and J. Xu, "26 m/5.5 gbps air-water optical wireless communication based on an ofdm-modulated 520-nm laser diode," *Optics express*, vol. 25, no. 13, pp. 14 760–14 765, 2017.

[9] P. Nabavi, A. F. M. S. Haq, and M. Yuksel, "Empirical modeling and analysis of water-to-air optical wireless communication channels," in *IEEE Int. Conference on Communications Workshops*, 2019, pp. 1–6.

[10] S. Karp, "Optical communications between underwater and above surface (satellite) terminals," *IEEE Transactions on Communications*, vol. 24, no. 1, pp. 66–81, 1976.

[11] Y. Dong, S. Tang, and X. Zhang, "Effect of random sea surface on downlink underwater wireless optical communications," *IEEE communications letters*, vol. 17, no. 11, pp. 2164–2167, 2013.

[12] N. Huang, C. Gong, C. Fu, T. Wei, and Z. Xu, "Preliminary investigation of air-to-water visible light communication link under strong ambient light," in *IEEE Vehicular Tech. Conf.*, 2021, pp. 1–5.

[13] A. Wang, L. Zhu, Y. Zhao, S. Li, W. Lv, J. Xu, and J. Wang, "Adaptive water-air-water data information transfer using orbital angular momentum," *Optics express*, vol. 26, no. 7, pp. 8669–8678, 2018.

[14] L.-K. Chen, Y. Shao, and Y. Di, "Underwater and water-air optical wireless communication," *Journal of Lightwave Technology*, 2021.

[15] S.-C. Tu, Y.-C. Huang, and H.-H. Lu, "256 gb/s four-channel sdm-based pam4 fso-uwoc convergent system," in *IEEE Photonics Conference*, 2019, pp. 1–2.

[16] Y. Shao, R. Deng, J. He, K. Wu, and L.-K. Chen, "Digital 4k video transmission over realtime water-air owc-ofdm system with low-complexity transmitter-side dsp," in *IET European Conference on Optical Communication*, 2019, pp. 1–4.

[17] X. Sun, M. Kong, C. Shen, C. H. Kang, T. K. Ng, and B. S. Ooi, "On the realization of across wavy water-air-interface diffuse-line-of-sight communication based on an ultraviolet emitter," *Optics Express*, vol. 27, no. 14, pp. 19 635–19 649, 2019.

[18] P. Agheli, H. Beyranvand, and M. J. Emadi, "Uav-assisted underwater sensor networks using rf and optical wireless links," *Journal of Lightwave Technology*, vol. 39, no. 22, pp. 7070–7082, 2021.

[19] K. Enhos, E. Demirors, D. Unal, and T. Melodia, "Software-defined visible light networking for bi-directional wireless communication across the air-water interface," in *IEEE International Conference on Sensing, Communication, and Networking (SECON)*, 2021, pp. 1–9.

[20] T. Lin, N. Huang, C. Gong, J. Luo, and Z. Xu, "Preliminary characterization of coverage for water-to-air visible light communication through wavy water surface," *IEEE Photonics Journal*, vol. 13, no. 1, pp. 1–13, 2021.

[21] M. Davies and A. K. Chattopadhyay, "Stokes waves revisited: Exact solutions in the asymptotic limit," *The European Physical Journal Plus*, vol. 131, no. 3, pp. 1–5, 2016.

[22] Z. Song, H. Zhao, L. Li, and G. Lü, "On the universal third order stokes wave solution," *Science China Earth Sciences*, vol. 56, no. 1, pp. 102–114, 2013.

[23] A. Toffoli, A. Babanin, M. Onorato, and T. Waseda, "Maximum steepness of oceanic waves: Field and laboratory experiments," *Geophysical Research Letters*, vol. 37, no. 5, 2010.